EPSC Abstracts
Vol. 12, EPSC2018-1171, 2018
European Planetary Science Congress 2018

The Radar and Visible Stratigraphic Records of Mars' North Polar Layered Deposits

P. Becerra (1), D. Nunes (2), I. Smith (3), M.M. Sori (4), Y. Brouet (1), N. Thomas (1)
(1) Physikalisches Institut, Universität Bern, Switzerland (2) Jet Propulsion Laboratory, Pasadena, California, USA (3) Planetary Science Institute, Boulder, CO, USA. (4) University of Arizona, Tucson, AZ, USA.

Abstract

We present an initial correlation of visible imagery and stereo-topography from HiRISE and sub-surface radar from SHARAD of Mars' NPLD. Resulting stratigraphic columns can constrain NPLD formation models to explore a connection to Mars' climate.

1. Introduction

A long-standing problem in Mars Polar Science is the interpretation of the stratigraphic record preserved in Mars' icy North Polar Layered Deposits (NPLD) [1] (Fig. 1a), whose accumulation patterns of ice and dust are associated with recent climatic changes forced by variations in the planet's astronomical parameters [2]. The internal bedding is visible from orbit in exposures within spiraling troughs that dissect the NPLD dome (Fig. 1a,b). Studies have used remote images of these troughs to map the stratigraphy [3-6] and search for a connection between NPLD accumulation and astronomical forcing [7-10]. Sub-surface radar sounding also observes this internal structure. The Shallow Radar (SHARAD) [11] detects changes in dielectric properties with depth. As these vary for layers with different amounts of dust contamination, layering is observed in the radar data as "reflector" surfaces [12].

The optical and radar-based stratigraphies have predominantly been studied in isolation. In terrestrial climate science [13], orbital climate forcing was ultimately confirmed by the correlation of sedimentary, geochemical and paleo-magnetic records, suggesting that integration of datasets is key to understanding the climate record of the NPLD. In general, both radar and optical layers are assumed to result from varying amounts of dust impurities in the ice [14], which was supported by [15], who in attempting the first quantitative correlation between these data found an agreement between large-scale properties of radar reflectors and visible layers. The unique correlation of a particular radar reflector with one exposed bed or packet remains an open problem.

Here, we present our approach to this correlation. We test the hypothesis that highly protruding 'Marker Beds (MBs)' have sufficient dielectric contrast with neighboring beds to create radar reflections. If true, this would associate individual reflectors to exposed beds, allowing for the construction of dust/ice columns based on the combined data. These could then constrain orbitally-forced accumulation models [16,17] that could unlock the temporal climate record of the NPLD.

2. Methods

Becerra et al. [8] mapped the stratigraphy of the NPLD by identifying sequences of MBs in "protrusion profiles" of bed exposures in troughs made from HiRISE [18] Digital Terrain Models (DTMs; [19]), and correlating these from different locations (Fig. 1; [8]). We take advantage of this work, and take the following approach:
(1) *Average SHARAD data near the exposures to obtain representative radargrams.* The variability of the SHARAD subsurface response within small regions of interest (ROIs) next to exposure sites must be taken into account. To assess this, we selected segments of three SHARAD radargrams that fall within a 3 km ROI near N0, and averaged all soundings contained in each segment (Fig. 2). Two have similar responses at the range of interest (blue and green), and one does not (red). This is representative of the variations in radar response observed within the ROI.
(2) *Compare average radargrams directly to the protrusion profiles of* [8] *to search for an MB-reflector correlation*. For this, we subtract the linear attenuation in the data and normalize all quantities to mean = 0 and variance = 1. We then search for the maximum cross-correlation between protrusion profiles and average radargrams.
(3) *Model the radar wave propagation (following* [15]*) through synthetic permittivity (ε) profiles.* These would be constrained by the best-fit correlations from step 2, such that MBs translate into layers of high ε. We test a preliminary version of the model, in which we select specific MBs from the N0 profile and assign them ε = 4, over a water ice background with ε = 3.12. We then compare the model radargrams to the real ones from each location. Fig. 3 shows the dielectric profile (center) modeled

after the protrusion profile (left) of site N0, and the resulting simulated radargram (right).

(4) *Correlate the simulated radargrams to real SHARAD data using spectral analysis and pattern-matching algorithms.* This correlation will result in representative HiRISE/SHARAD-based stratigraphic columns of ε, which can be transformed to fractional dust-content [20,21] that can serve as virtual ice cores and be used to constrain accumulation models.

3. Preliminary Results

Results of the cross-correlation of SHARAD with the protrusion profiles and model radargrams for site N0 are shown in Fig 4. For the direct comparison with protrusion we select only the sections of the radargrams that correspond to the estimated relevant depth range [2–8 ms], while the comparison with the models includes the surface reflection and an "overburden" [0–8 ms]. In the former, the blue and green radargrams show good matches between reflectors and protrusion peaks, and while the red does not, lags of maximum correlation are similar for all three. In the latter, not all three radargrams showed similar maximum-correlation lags: The blue and green matches are close to what would be expected, while the red correlation fails.

4. Conclusions and Future Work

Beds of high protrusion appear to match radar reflectors at site N0, showing that this method is the correct approach to this problem. However, variability within the radar data must be taken into account. We must also study all geometrically favorable locations and test for statistical significance at each one. In addition, we will use the correlations with protrusion to inform the model and then use Dynamic Time Warping [7,22] to tune the model and find the best-fit dielectric profile at each site. The final step of the work will be to transform these profiles into dust/ice ratio columns [20,21] for use as input on accumulation models [17].

5. Figures

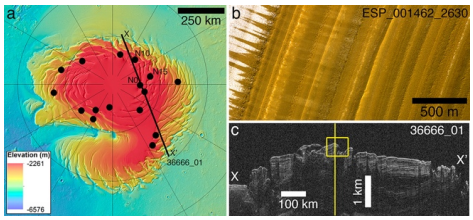

Figure 1. (a) Topographic map of the NPLD. Dots = locations of study sites and HiRISE DTMs [9]. Line is the ground track of the SHARAD radargram in (c). (b) HiRISE image of exposed layers in an NPLD trough. (c) SHARAD radargram (X-X' in 1a). Square marks the location of site N0. The line shows the position of the profiles of Fig. 2.

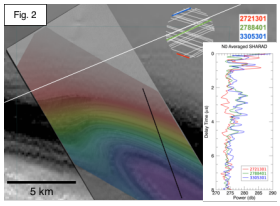

Figure 2. Zoom view of site N0. ROI for radargram averaging in top right. Plot of each average radargram.

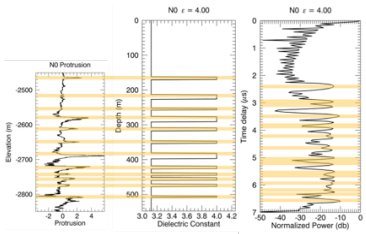

Figure 3. N0 protrusion profile (left) used to build a dielectric profile (center), through which a model radar wave is propagated to obtain a simulated radargram (right).

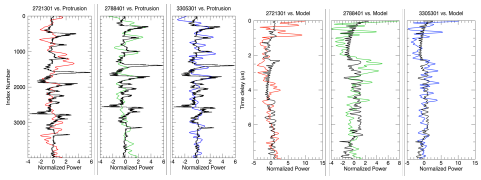

Figure 4. Cross-correlation of N0 average radargrams with N0 protrusion (left) and simulated radargrams (right).

Acknowledgements

This work is funded by Swiss National Science Foundation grant number 200020_178847. We thank the HiRISE and SHARAD Science and Operations team for the acquisition of the data and production of the DTMs.

References

[1] Smith, et al. *Icarus* (2018) [2] Cutts, et al. *Science* (1976) [3] Fishbaugh et al. (2006) [4] Fishbaugh et al. *GRL* (2010) [5] Limaye et al. *JGR* (2012) [6] Becerra et al. *JGR* (2016) [7] Laskar et al. *Nature* (2002) [8] Milkovich and Head, *JGR* (2005) [9] Perron and Huybers, *Geology* (2009) [10] Becerra et al. *GRL* (2017) [11] Seu et al. *JGR* (2007) [12] Putzig et al. *Icarus* (2009) [13] Imbrie, *Icarus* (1982) [14] Nunes & Phillips, *JGR* (2006) [15] Christian, et al. *Icarus* (2013) [16] Levrard et al. JGR (2007) [17] Hvidberg et al. *Icarus* (2012) [18] McEwen et al. JGR (2007) [19] Kirk et al. JGR (2008) [20] Stillman, et al. *J.Phys.Chem.* (2010) [21] Brouet et al. *(in prep.)* [22] Sori et al. Icarus (2014).